
Informed Correctors for Discrete Diffusion Models

Yixiu Zhao
Stanford University
yixiuz@stanford.edu

Jiaxin Shi
Google DeepMind
jiaxins@google.com

Lester Mackey
Microsoft Research New England
lmackey@microsoft.com

Scott Linderman
Stanford University
scott.linderman@stanford.edu

Abstract

Discrete diffusion modeling is a promising framework for modeling and generating data in discrete spaces. To sample from these models, different strategies present trade-offs between computation and sample quality. A predominant sampling strategy is predictor-corrector τ -leaping, which simulates the continuous time generative process with discretized predictor steps and counteracts the accumulation of discretization error via corrector steps. However, for absorbing state diffusion, an important class of discrete diffusion models, the standard forward-backward corrector can be ineffective in fixing such errors, resulting in subpar sample quality. To remedy this problem, we propose a family of informed correctors that more reliably counteracts discretization error by leveraging information learned by the model. For further efficiency gains, we also propose k -Gillespie’s, a sampling algorithm that better utilizes each model evaluation, while still enjoying the speed and flexibility of τ -leaping. Across several real and synthetic datasets, we show that k -Gillespie’s with informed correctors reliably produces higher quality samples at lower computational cost.

1 Introduction

Denoising diffusion models are powerful generative models for high-dimensional data [1–3]. The central idea of diffusion models is to gradually corrupt data into noise using a “noising” or “forward” process and then to train a parameterized model (usually a deep neural network) to learn its time reversal, commonly known as the “denoising” or simply the “backward” process. In continuous domains such as image generation, the forward process is usually defined by gradual injection of Gaussian noise and scaling, transforming the data distribution close to a standard normal. The backward process is then approximated by learning the gradient of the log density (also known as the “score function”) of the marginal distribution. Samples can be drawn from a trained model by first generating Gaussian noise and then simulating the backward process using the score information. Diffusion generative models are currently the dominant framework for image generation and can generate high-resolution images with stunning details and style given prompts by the users [4, 5].

Given the success of diffusion models in continuous domains, recent work has explored diffusion modeling in discrete domains [6–13], with applications to language [13], protein sequences [14, 15], graphs [16], and more. Notably, Campbell et al. [9] developed TauLDR, a general framework for discrete denoising diffusion in continuous time. They formulated the forward and backward processes as continuous time Markov chains (CTMCs), and their model learns to predict the distribution over denoised data via an evidence lower bound (ELBO) objective. Lou et al. [13] adopted a very similar strategy but instead directly parameterize the concrete score function — an analog of the continuous score function in discrete spaces.

Despite the conceptual progress on discrete diffusion, many challenges in implementation still limit the effectiveness of these models. One major challenge lies in the trade-off between efficiency and accuracy in simulating the continuous-time backward process. Song et al. [17] proposed using approximate MCMC correctors to correct for the discretization error in simulating diffusion backward process. Campbell et al. [9] extended predictor-corrector sampling to discrete diffusion models and discovered that the corrector steps significantly impact generative performance. However, a clear understanding of how the choice of corrector steps influences sample quality is still lacking.

Can further gains be made from leveraging different sampling methods? We give an affirmative answer. By analyzing the forward-backward corrector used in TauLDR, we identify failure modes in absorbing state diffusion and develop a simple synthetic “countdown” dataset that exposes the pathologies of standard corrector steps. To address this shortcoming:

- We propose a family of “informed correctors” and accompanying training schemes that further capitalize on the score information gathered by the model during training. We use them to guide the sampling process, correcting mistakes and accelerating mixing.
- We propose an alternative to τ -leaping called k -Gillespie’s, which takes a fixed number of updates $k \geq 1$ per backward step. We show that it generally achieves better sample quality than τ -leaping for the same number of model evaluations.

We compare these models on the countdown dataset as well as benchmarks for discrete sequence generation including gene expression the monophonic music sequences, We show that informed correctors, together with our other algorithmic and architectural proposals, produce higher quality samples with fewer model evaluations.

2 Background

2.1 Continuous-Time Discrete Diffusion Models

Consider a data point $x_0 \in \mathcal{S}$ which is assumed to be sampled from the data distribution $p_{\text{data}}(x_0)$. Denoising diffusion models [1–3] seek to model this unknown data distribution by progressively adding noise to data samples until their distribution converges to a simple target, such as a uniform distribution. Then, a deep neural network is trained to invert this process and remove the noise. This reverse process forms a generative model from which new samples can be drawn. The noising and generative processes are also called the *forward* and *backward* processes, respectively. We will adopt this convention for the rest of the paper.

Continuous-time diffusion models define a forward process with noising distribution $q_t(x_t|x_0)$ and marginals $q_t(x_t) = \int q_t(x_t|x_0)q_0(x_0)dx_0$, with $q_0 = p_{\text{data}}$ and $q_T \approx \pi$ where π is the limiting distribution of the forward process, which is assumed to be a simple distribution. Then, a parameterized process with marginals p_t^θ is learned to match the true backward process.

When the data of interest is discrete in nature (e.g., text, protein sequences, neural spike counts), the forward-process can be described with a continuous-time Markov chain (CTMC), which is captured by the initial distribution q_0 and a transition rate matrix $R_t \in \mathbb{R}^{S \times S}$, where $S = |\mathcal{S}|$ denotes the cardinality of the data space. The off-diagonal terms $R_t(x, y), x \neq y$ of the matrix represent the rate of state x transitioning to state y , and the diagonals $R_t(x, x)$ are defined as the negative sum of all other elements in the same row: $R_t(x, x) = -\sum_{y \neq x} R_t(x, y)$. Under the assumption that R_s and R_t commute for all s and t , the finite-time transition probabilities satisfy

$$q_{t+\Delta t|t}(y | x) = \left[\exp \left\{ \int_t^{t+\Delta t} R_s ds \right\} \right] (x, y) = I(x, y) + R_t(x, y)\Delta t + o(\Delta t), \quad (1)$$

where I represents the identity matrix, and in the square brackets we compute a matrix exponential. It can then be shown [9] that the time reversal of the above CTMC is another CTMC with the transition rate

$$\tilde{R}_t(y, x) = R_t(x, y) \frac{q_t(x)}{q_t(y)} = R_t(x, y) \sum_{x_0} \frac{q_{t|0}(x | x_0)}{q_{t|0}(y | x_0)} q_{0|t}(x_0 | y). \quad (2)$$

Campbell et al. [9] approximate the backward rate by learning a parameterized denoising model $p_{0|t}^\theta(x_0 | y) \approx q_{0|t}(x_0 | y)$. Alternatively, Meng et al. [18] and Lou et al. [13] observed that the

ratio $s_t(y)_x \triangleq q_t(x)/q_t(y)$ plays a similar role as the continuous score function $\nabla \log q_t(y)$, up to an additive constant. Therefore, they proposed to learn an approximate function, $s_t^\theta(y)$. We adopt the denoising parameterization of Campbell et al. [9] in our work, but use both of these objects in our exposition, keeping in mind the relationship between them:

$$s_t^\theta(y)_x = \sum_{x_0} \frac{q_{t|0}(x | x_0)}{q_{t|0}(y | x_0)} p_{0|t}^\theta(x_0 | y). \quad (3)$$

Regardless of the parameterization, the training objective can be given by the variational lower bound of the data log likelihood in terms of the parameterized backward rate $\tilde{R}_t^\theta(y, x) = R_t(x, y) s_t^\theta(y)_x$:

$$-\log p(x_0) \leq \mathcal{L}(\theta) = \int \mathbb{E}_{q_{t|0}(y|x_0)} \left[\sum_{x \neq y} \left\{ \tilde{R}_t^\theta(y, x) - R_t(x, y) \frac{q_{t|0}(x | x_0)}{q_{t|0}(y | x_0)} \log(\tilde{R}_t^\theta(y, x)) \right\} \right] dt + C, \quad (4)$$

where C is a constant independent of θ . This is the standard evidence lower bound (ELBO) objective for training continuous time discrete diffusion models.

Note that this objective is superficially different from the one in Campbell et al. [9], which practically requires two Monte Carlo samples to estimate instead of one. However, as Shi et al. [19] have noted, these objectives are mathematically equivalent, therefore we present the simpler form here. We provide a derivation of this fact in Appendix A and refer readers to Shi et al. [19] for more detail. In practice, we choose the objective that matches existing work for fair comparison.

2.2 Sequence Modeling with the Absorbing Forward Process

For real-world applications, the data is often a vector or sequence $x^{1:D}$ of length D , where each dimension of the data x^d belongs to a vocabulary, and the full state space is the product of the vocabularies and thus exponentially large. With a shift in notation, we now use $\mathcal{S} = \{1, \dots, S\}$ to denote the ‘‘vocabulary’’ set instead, whereas the full space is represented as \mathcal{S}^D .

Given the factorization of this space, it is natural to model the forward process as a composition of identical independent processes on each dimension, where the rate over the entire state R_t can be written as

$$R_t(x, y) = \beta(t) \sum_d R_b(x^d, y^d) \mathbb{1}_{\{x^d = y^d\}} \quad (5)$$

for a base rate matrix $R_b \in \mathbb{R}^{\mathcal{S} \times \mathcal{S}}$, absorbing the time dependence into the scalar coefficient $\beta(t)$. With this factorization of the forward rate, the backward rates are also factorized, but now with a different time-dependent rate \tilde{R}_t^d for each dimension d . This means that the objective in (4) can be decomposed nicely into a sum over dimensions, as detailed by Campbell et al. [9].

For generic discrete data, two forward processes are most commonly used: the uniform process and the absorbing state process. We focus on the absorbing state process in this paper, for which the base rate matrix for each dimension can be written as

$$R_b^{\text{absorb}}(x, y) = \begin{cases} 1 & y = \text{MASK}, x \neq \text{MASK} \\ -1 & y = x, x \neq \text{MASK} \\ 0 & \text{otherwise,} \end{cases} \quad (6)$$

where we augment the vocabulary set \mathcal{S} by introducing the MASK token, which represents the absorbing state. The absorbing state diffusion is important to consider because it is very commonly used to model sequence data without ordinal structure (e.g., text and protein sequences). It is also intimately connected to masked language models [8, 20, 21].

We use special notation for the absorbing state process. For a sequence $x \in \{\text{MASK}, 1, \dots, S\}^D$, we use the mask operator $y = M^d(x)$ to denote the sequence obtained by changing the d th component of x to MASK. Finally, we denote the masked indices of x by $\mathcal{M}(x) \equiv \{d : x^d = \text{MASK}\}$. Then the set of non-mask indices is denoted by the set complement $\overline{\mathcal{M}}(x)$.

2.3 Sampling From the Backward Process

Gillespie’s method Given learned rates \tilde{R}_t^θ for the backward process, one can approximately sample from the backward Markov jump process using Gillespie’s algorithm [22] which computes

holding times at the current state, and recomputes the backward rates after the holding time has passed and a state change takes place. The approximation arises when the backward rates are treated as constant over short time intervals, when they in fact change continuously in time. Gillespie’s algorithm changes a single component of the state at a time, which is computationally expensive for generating high-dimensional data.

Tau leaping Instead, Campbell et al. [9] proposed to use τ -leaping, an approximate sampling method that allows simultaneous updates to multiple dimensions for a single model evaluation. τ -leaping assumes that the backward process transition rate is constant between $[t - \tau, t)$, regardless of whether states change during that interval. Under this assumption, the number of transitions in the interval is a Poisson random variable, and several transition events can be applied simultaneously.

2.4 Corrector Steps for τ -leaping

Because of the approximate nature of the τ -leaping steps, this approach accumulates simulation errors over the course of the backward process. To combat this problem, additional corrector steps can be used to make sure that the marginal distribution of samples x_t at time t matches q_t . Campbell et al. [9] show that a corrector process with rates:

$$R_t^c(x, y) = R_t(x, y) + \tilde{R}_t(x, y) \tag{7}$$

leaves the stationary distribution q_t invariant. In practice, one must use the learned backward rates \tilde{R}_t^θ as an approximation for the true backward rates \tilde{R}_t . We refer to this as the forward-backward corrector, as it is simply a summation of the forward and backward rates. Campbell et al. [9] demonstrate that the forward-backward corrector increases sample quality in practice.

Correcting for the absorbing diffusion The necessity of corrector steps is particularly apparent when τ -leaping is used in conjunction with an absorbing forward process. In the reversal of the absorbing process, only transitions from the absorbing state to other states are allowed, which is reflected by the structure of \tilde{R}_t . Thus, once a token has been generated, it cannot be erased or changed, rendering it impossible for the predictor to fix its own errors. Forward-backward corrector steps mitigate this issue by introducing the forward term R_t , allowing transitions in the forward direction, resulting in generated tokens being “masked out” again with uniform probability.

Though forward-backward corrector steps solve the issue in theory, we note that the forward-backward corrector is far from optimal in practice. It can only correct mistakes by masking them at random. Ideally, we would like the corrector to make informed transitions based on which states are more likely under the model. This observation motivates us to find a better alternative to the forward-backward corrector.

3 Methods

This section presents our main contributions. Focusing on discrete diffusion models with an absorbing forward process, we propose a modification of Gillespie’s algorithm, a classic algorithm for simulating CTMCs, to approximate the backward process with fewer model evaluations. Then, motivated by the discussion above, we develop novel corrector steps for the reverse process. Taking inspiration from the Stein operator literature, we present informed correctors, a family of Markov transition operators that leverage score information learned by the model to more efficiently address mistakes in the reverse process and improve sample quality.

3.1 k -Gillespie’s Algorithm

In the absorbing state reverse process, a change in the state happens if and only if a new token is generated from the absorbing state. This means that the number of state changes is exactly equal to the number of positions D , which, in Gillespie’s algorithm, also corresponds to D model evaluations.

Unlike Gillespie’s, τ -leaping can freely choose the number of model evaluations by changing the step size τ . This enables a trade-off between sample quality and computation. Unfortunately, a Poisson-distributed number of updates in the τ -leaping algorithm means that on some steps, no

updates are made at all. One model evaluation can lead to multiple coordinates being updated at once — a loss of accuracy — or no coordinates being updated at all — a loss of efficiency.

To address this issue with τ -leaping, we propose a simple modification of Gillespie’s algorithm. A single model evaluation provides information about transition rates for all dimensions D . Rather than updating only the dimension with the smallest holding time, we update the $k \geq 1$ dimensions with the smallest holding times simultaneously. By approximating the rate as constant within the time of these k transitions, this allows us to generate samples using only $\lfloor \frac{D}{k} \rfloor$ model evaluations. Similar to τ -leaping, we can also offset the accumulation of errors due to this approximation by applying corrector steps after each set of updates. We provide pseudo-code for this in Algorithm 1 in the appendix.

3.2 Informed Correctors

We propose the following family of correctors for discrete diffusion sampling by combining the symmetrized forward process and with an additional “corrector operator,” A_t ,

$$R_t^c(x, y) = \begin{cases} (R_t(x, y) + R_t(y, x)) \cdot A_t(x, y) & x \neq y \\ -\sum_z R_t^c(x, z) & x = y \end{cases} \quad (8)$$

Here, A_t is the matrix representation of a Markov transition operator that leaves the marginal distribution q_t invariant. That is, a continuous time Markov jump process generated by A_t has stationary distribution q_t . One way to obtain a corrector operator is by appealing to the literature on Stein operators. For example, a Zanella Stein operator [23] is of the form,

$$A_t(x, y) = \begin{cases} \kappa\left(\frac{q_t(y)}{q_t(x)}\right) & y \neq x \\ -\sum_z A_t(x, z) & y = x \end{cases}, \quad (9)$$

where κ is a positive function satisfying $\kappa(t) = t\kappa(1/t)$.¹ In this work, we will focus on the minimum probability flow (MPF) Stein operator [24, 25], where $\kappa(t) = \sqrt{t}$, and the Barker Stein operator [26, 27], where $\kappa(t) = \frac{t}{t+1}$, two examples of Zanella Stein operators that have been found to work well in practice [26].

In practice, we would like to use A_t^θ to approximate A_t , where A_t^θ uses the learned concrete score s_t^θ in place of the true s_t . However, it is important to note that this approximation is not always viable, since the score information $\frac{q_t(x)}{q_t(y)}$ is not learned by the model for all pairs of (x, y) , but only for those that are allowed by the forward process. This follows from the ELBO objective in (4), where the learning signal is weighted by the forward rates. Therefore, the model can learn poor approximations for $\frac{q_t(x)}{q_t(y)}$ if the forward rate $R_t(x, y)$ is 0 or very small.

While diffusion with a uniform forward process is not affected by virtue of sampling transitions between all pairs of states during training, this limitation becomes apparent for absorbing state diffusion, which only allows mask to non-mask transitions but not vice versa. In the next section, we show why having informed correctors is especially important in the absorbing case and illustrate ways to learn informed correctors with small adjustments to the score function architecture.

4 Learning Informed Correctors for Absorbing State Diffusion

We develop an approach for learning informed correctors for discrete diffusion models with absorbing forward processes. Specifically, we modify the parameterization and architecture such that when trained with the *same* ELBO objective, the model learns the necessary score information efficiently. Note that this change in architecture is only required for the absorbing state diffusion, and for uniform process diffusion informed correctors can be applied directly without changing the learning scheme.

4.1 Alternative Parameterization for Efficient Score Evaluation

The corrector rates in (8) and (9) provide a nonzero rate of converting the token at the d -th dimension of x back into a mask. These rates depend on the score function $s_t(x)_{M^d(x)} \triangleq q_t(M^d(x))/q_t(x)$.

¹Zanella [23] defines a neighborhood of state x , but premultiplying by the symmetrized forward rate matrix $R_t(x, y) + R_t(y, x)$ achieve a similar effect, allowing us to simplify the presentation of A_t .

However, $s_t^\theta(x)_{M^d(x)}$ is not learned because $R_t(M^d(x), x) = 0$ which zeros out the reverse rate \tilde{R}_t^θ in (4). We can circumvent this issue by inverting the learned score $s_t^\theta(M^d(x))_x$ to get the desired ratio. Nevertheless, this approach is very computationally inefficient: to compute the transition rates for all non-mask dimensions, we need to evaluate our model on $|\overline{\mathcal{M}}(x)|$ different inputs.

We address this challenge via an alternative parameterization of the denoising model. Let $f^\theta(x, t)$ represent a neural network that implements an approximate denoising distribution. It takes in an observation x and time t and outputs a tensor in $\mathbb{R}^{D \times S}$. Let $f^\theta(x, t)_{d,i}$ denote the (d, i) -th output of the neural network, which represents the denoising probability $p_{0|t}^\theta(x_0^d = i | x) \triangleq f^\theta(x, t)_{d,i}$.

For an absorbing process, observe that for $d \in \overline{\mathcal{M}}(x)$ we know that $q_{0|t}(x_0^d = i | x) = \mathbb{1}_{\{x^d=i\}}$, which implies that the entire output probability vector $f^\theta(x, t)_{d,:}$ is unused. We propose to use these output dimensions to approximate $q_{0|t}(x_0^d | M^d(x))$ instead. With that information, we can compute the required score information via,

$$s_t(x)_{M^d(x)} = \left(\frac{q_t(x)}{q_t(M^d(x))} \right)^{-1} \approx \left[\sum_{i=1}^S \frac{q_{t|0}(x | x_0 = i)}{q_{t|0}(M^d(x) | x_0 = i)} f^\theta(x, t)_{d,i} \right]^{-1}. \quad (10)$$

To summarize, for $d \in \mathcal{M}(x)$, the network outputs the same denoising distribution as before; for $d \in \overline{\mathcal{M}}(x)$, the network operates as if the input has a mask token at dimension d . With this parameterization, a single function evaluation is sufficient for computing the informed corrector rates for all D dimensions.

4.2 Learning the Full Score Information Using Hollow Transformers

Despite the conceptual simplicity, for this parameterization to work in practice, one must make sure that for $d \in \overline{\mathcal{M}}(x)$ information about x^d does not leak to the output $f^\theta(x, t)_{d,i}$. To achieve this, we use a hollow transformer [28], a two-stream self-attention architecture where each stream runs causal attention in a different direction. The embeddings are then offset by one position so that the embedding at position d does not attend to the corresponding input position. By combining these two directional streams, the hollow transformer satisfies the property that, for continuous x ,

$$\frac{\partial}{\partial x^d} f_{HT}^\theta(x, t)_{d,i} = 0 \quad \forall i \in \{1, \dots, S\}. \quad (11)$$

In other words, the network output at dimension d is agnostic to the input at the same dimension d . We provide more details of the model architecture in Section 6.

Learning the Hollow Transformer with the ELBO Objective The parameterization in (10) can be learned with the hollow transformer without changing the ELBO objective (4). To see why, consider a pair of observations x and $x' = M^d(x)$ such that $x^d \neq \text{MASK}$. By the property of the hollow transformer, $f_{HT}^\theta(x, t)_{d,i} = f_{HT}^\theta(x', t)_{d,i}$. However, since the forward rate $R_t(\cdot, x)$ is 0 under the absorbing forward process, the backward rate $\tilde{R}_t^\theta(x, \cdot)$ is also 0. This means that during training, gradients only flow through $\tilde{R}_t^\theta(\mathcal{M}^d, \cdot)$, which encourages the network output $f_{HT}^\theta(x, t)_{d,i}$ to approach the true denoising distribution $q_{0|t}^\theta(x_0^d = i | M^d(x))$ which is conditioned on the masked state $M^d(x) = x'$. In other words, since the model does not see x^d when producing the output at dimension d , it always tries to produce outputs as if $x^d = \text{MASK}$ to minimize the loss.

5 Related Work

Discrete diffusion models and predictor-corrector sampling. Sohl-Dickstein et al. [1] derived a discrete diffusion model but only for binomial variables. Hoogeboom et al. [6], Song et al. [7] extended the formulation to categorical variables using a uniform noising distribution, which was further generalized by Austin et al. [8] to enable any corruption processes specified with a transition matrix. Austin et al. [8] also discussed the continuous-time limit of the proposed discrete diffusion model. A continuous-time objective amenable to training was first proposed by Campbell et al. [9] and further developed by Benton et al. [12], Lou et al. [13], Shi et al. [19]. In addition to this line of

work on formally defining the forward and backward diffusion process and deriving likelihood-based training objectives, there is also a family of diffusion-inspired models targeted at discrete data, such as SUNDAE [29], MaskGIT [30], and SDDM [28]. These models are typically trained by an objective that does not necessarily correspond to maximizing the likelihood of data, such as a (weighted) denoising loss (i.e., cross-entropy for discrete data) or a generalization of ratio-matching losses [28]. The first use of predictor-corrector samplers appeared in Song et al. [17] for continuous diffusion models. Campbell et al. [9] used correctors to improve their τ -leaping samplers for discrete diffusion. Relatedly, Lezama et al. [31] also proposed a corrector scheme to improve MaskGIT sampling.

MCMC in discrete spaces. The design of our corrector scheme involves finding continuous-time Markov chains that keep our current-time marginals as the stationary distribution. This problem has largely been studied for designing MCMC algorithms in discrete spaces. The Barker and MPF correctors are inspired by recent work [26, 32] that uses Zanella’s informed MCMC kernels [23] to construct Stein operators or transition rate matrices that have a target stationary distribution. In addition to the locally balanced proposals studied in Zanella [23], there are several other discrete MCMC kernels relying on continuous relaxation and combining ideas from Gibbs or Langevin samplers [33–35] which would be interesting to explore as correctors for discrete diffusion models in future work.

6 Experiments

We evaluate k-Gillespie’s algorithm and informed correctors on synthetic and real datasets for both unconditional and conditional sampling tasks. We train a hollow transformer architecture augmented for denoising diffusion using standard implementation techniques [17]. The inputs to the transformer are treated as one-hot variables, destroying all ordinal structure of the data. Our networks use 5M to 8M parameters depending on the task. Training is done using a single A100 GPU with 80GB of memory on an academic cluster.

To study efficiency-quality trade-offs, we measure different dataset-dependent metrics and also record the number of function evaluations (NFE) needed to produce each sample under different sampling schemes. For τ -leaping, we control NFE via tuning the τ parameter, which is the inverse of the number of predictor steps. For our k -Gillespie’s, we change k from 1 to 3, with higher values of k resulting in fewer NFEs. Keep in mind that each corrector step also requires one function evaluation.

6.1 The Countdown Dataset

To check our intuition that standard forward-backward correctors would perform poorly for absorbing diffusion processes (see Section 2.4), we create a synthetic sequence dataset with strong position-wise correlation structure and test generation quality for different corrector steps. Given a state size S and sequence length D , a data sequence $x^{1:D}$ is drawn according to the following rule:

$$x^1 \sim \text{Uniform}\{1, \dots, S\}, \quad x^{d+1} \mid x^d \sim \begin{cases} \delta_{x^d-1} & x^d \neq 0 \\ \text{Uniform}\{1, \dots, S\} & x^d = 0 \end{cases}. \quad (12)$$

We evaluate sample quality for this dataset using the error rate measured by the proportion of generated tokens that fail to count downward from the previous token:

$$r_{err}(\{\hat{x}_n\}_{1\dots N}) = \frac{1}{ND} \sum_{n=1}^N \sum_{d=1}^{D-1} \mathbb{1}_{\{\hat{x}_n^{d+1} \neq \hat{x}_n^d - 1\}} \mathbb{1}_{\{\hat{x}_n^d \neq 0\}}. \quad (13)$$

The results are shown in Figure 1. We confirm the observation from [9] that more corrector steps (thicker lines) improves sample quality. However, the forward-backward corrector (orange curves) notably benefits the least from increased corrector steps in proportion of errors. This confirms the intuition that the forward-backward corrector is bad at correcting mistakes due to masking tokens uniformly at random.

Except for the MPF corrector on the proportion of errors metric, k -Gillespie’s (solid curves) greatly outperforms τ -leaping across different setting, achieving better sample quality with fewer than half as many model evaluations. Notably, MPF (pink curves) outperforms other correctors by an order of magnitude in reducing errors. We demonstrate this visually in Figure 2.

6.2 Gene Expression Data

To test if these sampling schemes also capture correlations on real data, we use a gene expression time series dataset [36] and the evaluation metrics from Kerrigan et al. [37]. We quantize the values by binning them into $S = 64$ discrete bins and train our model on the discretized data. Kerrigan et al. [37] evaluates the quality of the generated sequences by computing point-wise statistics for each position along the sequence lengths and computes the mean squared error (MSE) of these statistics between the samples and true data.

Unfortunately, these point-wise metrics are ineffective at testing the correlation structure of individual sampled sequences, since they only measure marginal distributions on each sequence dimension. However, as we have demonstrated previously, correctors are needed to compensate for the predictor’s failures to capture dependencies in the data. In order to better test this, we calculate the point-wise metrics on the discrete cosine transform (DCT) of the sequences.

The results are shown in Figure 3. Each method uses 56 model evaluations and 2 corrector steps per predictor step. We find that k -Gillespie’s still reliably outperforms τ -leaping, while the MPF informed corrector yields the best performance on many metrics.

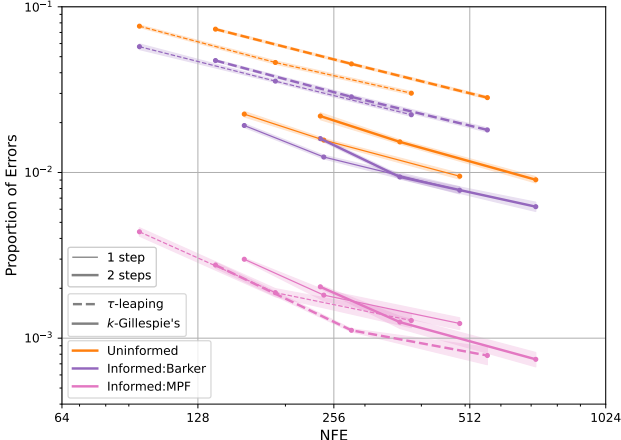


Figure 1: Comparison between different sampling schemes on the countdown dataset. The number of function evaluations is tuned by changing k and τ . Each run generates 500 sample sequences and standard deviations are computed from 5 runs with different random seeds.

6.3 Conditional Generation on Monophonic Music

Following Campbell et al. [9], we test conditional generation by modeling songs from the Lakh pianoroll dataset. In this dataset, monophonic sequences of length 256 are extracted, with each coordinate representing one of 128 notes or a rest. Campbell et al. [9] trained a discrete denoising diffusion model with the uniform forward process. The training objective was altered to target the last 224 time steps of the input sequence given the first 32. We construct our hollow transformer model with approximately the same number of parameters and train it for over 1M iterations.

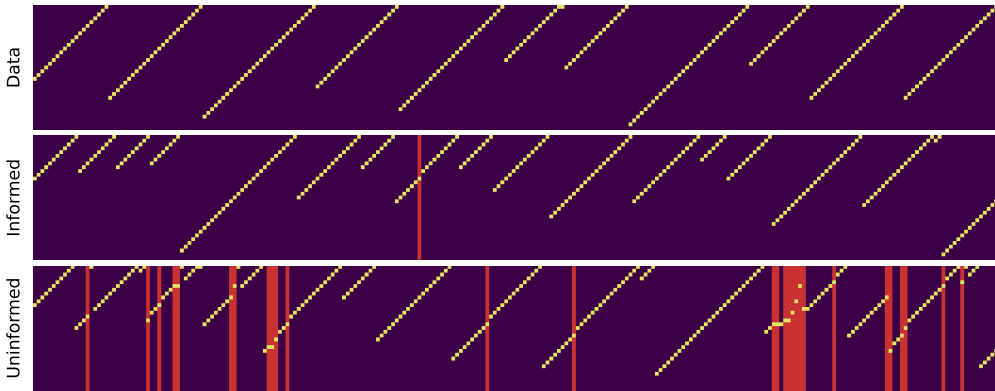


Figure 2: Samples taken using uninformed and informed correctors on the countdown dataset. The top row shows a typical data sequence. The middle sequence is sampled using k -Gillespie’s and the MPF corrector (NFE = 163), and the bottom sequence is sampled with τ -leaping and the forward-backward corrector (NFE = 190) with the same trained model. Positions with errors are marked by red. The uninformed corrector struggles with correcting errors in the sampling process.

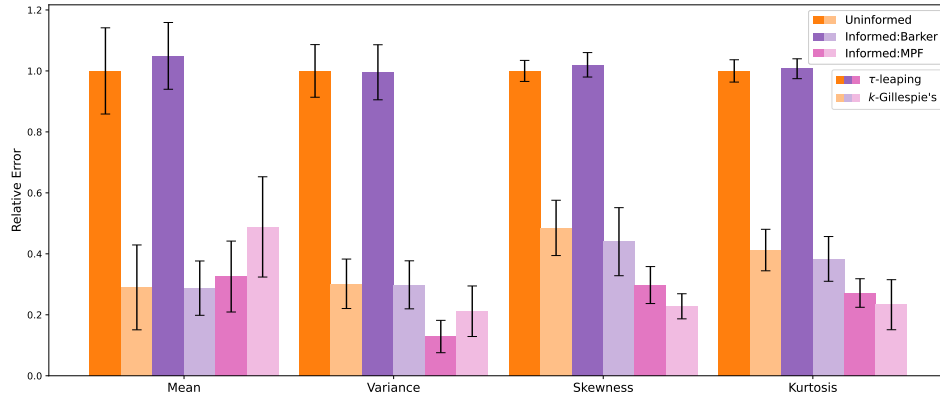


Figure 3: MSE for different pointwise statistics between the data and model samples, as compared to the baseline (τ -leaping with the forward-backward corrector). These statistics are evaluated on the discrete cosine transform of the sequence to better reflect correlation structure. The mean and standard deviations are shown for 20 runs of 500 samples each.

We report our best results in Table 1. The Hellinger distance is computed between the histograms of the generated and ground truth notes, and outliers are counted with the notes that are in the samples but not in the ground truth. We see that absorbing diffusion combined with k -Gillespie’s and the MPF corrector again generates high quality samples with only a fraction of the computational cost.

Table 1: Results on the monophonic piano dataset. The metrics are computed over the test set with 5 samples for each test sequence. The baseline results are taken from Campbell et al. [9]. For our results we use $\tau = 0.02$ and $k = 3$.

Method	NFEs	Hellinger Distance	Proportion of Outliers
τ -leaping + 2Uninformed (uniform)	2800	0.3762 ± 0.0015	0.1091 ± 0.0014
τ -leaping + 1Informed:MPF	95	0.3769 ± 0.0009	0.1231 ± 0.0011
k -Gillespie’s + 1Informed:MPF	142	0.3744 ± 0.0003	0.1071 ± 0.0010

7 Discussion

We proposed informed correctors and modified algorithms for discrete diffusion models with absorbing forward processes. We showed that common scheme of τ -leaping with the forward-backward corrector is not well-suited to this setting. To address this problem, we develop novel, informed correctors and provided a modified training strategy to learn them. We showed that this approach produces superior sample quality with fewer model evaluations than previous methods. Overall, our work serves to further enhance the capabilities of diffusion models in discrete regimes.

Limitations Using the informed correctors for absorbing diffusion requires architecture modifications such as using the hollow transformer. In practice, we cannot apply the correctors directly for pretrained models and have to retrain them from scratch. This limits the direct applicability of our methods.

Future work In developing the informed corrector, we observed that design decisions in the training and sampling phases can be strongly coupled. To leverage better sampling methods, the need for modifying the training setup naturally arises. Future work could explore this coupling in more depth, for example, by studying how the architecture and training objective can be further adapted to efficient sampling strategies.

References

- [1] Jascha Sohl-Dickstein, Eric Weiss, Niru Maheswaranathan, and Surya Ganguli. Deep unsupervised learning using nonequilibrium thermodynamics. In *International Conference on Machine Learning*, pages 2256–2265. PMLR, 2015.

- [2] Jonathan Ho, Ajay Jain, and Pieter Abbeel. Denoising diffusion probabilistic models. *Advances in Neural Information Processing Systems*, 33:6840–6851, 2020.
- [3] Yang Song and Stefano Ermon. Generative modeling by estimating gradients of the data distribution. *Advances in neural information processing systems*, 32, 2019.
- [4] Aditya Ramesh, Mikhail Pavlov, Gabriel Goh, Scott Gray, Chelsea Voss, Alec Radford, Mark Chen, and Ilya Sutskever. Zero-shot text-to-image generation. In *International Conference on Machine Learning*, pages 8821–8831. Pmlr, 2021.
- [5] Robin Rombach, Andreas Blattmann, Dominik Lorenz, Patrick Esser, and Björn Ommer. High-resolution image synthesis with latent diffusion models. In *Proceedings of the IEEE/CVF Conference on Computer Vision and Pattern Recognition*, pages 10684–10695, 2022.
- [6] Emiel Hoogeboom, Didrik Nielsen, Priyank Jaini, Patrick Forré, and Max Welling. Argmax flows and multinomial diffusion: Learning categorical distributions. *Advances in Neural Information Processing Systems*, 34:12454–12465, 2021.
- [7] Jiaming Song, Chenlin Meng, and Stefano Ermon. Denoising diffusion implicit models. In *International Conference on Learning Representations*, 2020.
- [8] Jacob Austin, Daniel D Johnson, Jonathan Ho, Daniel Tarlow, and Rianne Van Den Berg. Structured denoising diffusion models in discrete state-spaces. *Advances in Neural Information Processing Systems*, 34:17981–17993, 2021.
- [9] Andrew Campbell, Joe Benton, Valentin De Bortoli, Tom Rainforth, George Deligiannidis, and Arnaud Doucet. A continuous time framework for discrete denoising models. *arXiv preprint arXiv:2205.14987*, 2022.
- [10] Javier E Santos, Zachary R Fox, Nicholas Lubbers, and Yen Ting Lin. Blackout diffusion: Generative diffusion models in discrete-state spaces. *arXiv preprint arXiv:2305.11089*, 2023.
- [11] Lin Zheng, Jianbo Yuan, Lei Yu, and Lingpeng Kong. A reparameterized discrete diffusion model for text generation. *arXiv preprint arXiv:2302.05737*, 2023.
- [12] Joe Benton, Yuyang Shi, Valentin De Bortoli, George Deligiannidis, and Arnaud Doucet. From denoising diffusions to denoising markov models. *Journal of the Royal Statistical Society Series B: Statistical Methodology*, 86(2):286–301, 2024.
- [13] Aaron Lou, Chenlin Meng, and Stefano Ermon. Discrete diffusion language modeling by estimating the ratios of the data distribution. *arXiv preprint arXiv:2310.16834*, 2023.
- [14] Joseph L Watson, David Juergens, Nathaniel R Bennett, Brian L Trippe, Jason Yim, Helen E Eisenach, Woody Ahern, Andrew J Borst, Robert J Ragotte, Lukas F Milles, et al. De novo design of protein structure and function with RFdiffusion. *Nature*, 620(7976):1089–1100, 2023.
- [15] Sarah Alamdari, Nitya Thakkar, Rianne van den Berg, Alex Xijie Lu, Nicolo Fusi, Ava Pardis Amini, and Kevin K Yang. Protein generation with evolutionary diffusion: sequence is all you need. *bioRxiv*, pages 2023–09, 2023.
- [16] Clement Vignac, Igor Krawczuk, Antoine Siraudin, Bohan Wang, Volkan Cevher, and Pascal Frossard. Digress: Discrete denoising diffusion for graph generation. *arXiv preprint arXiv:2209.14734*, 2022.
- [17] Yang Song, Jascha Sohl-Dickstein, Diederik P Kingma, Abhishek Kumar, Stefano Ermon, and Ben Poole. Score-based generative modeling through stochastic differential equations. *arXiv preprint arXiv:2011.13456*, 2020.
- [18] Chenlin Meng, Kristy Choi, Jiaming Song, and Stefano Ermon. Concrete score matching: Generalized score matching for discrete data. *arXiv preprint arXiv:2211.00802*, 2022.
- [19] Jiaxin Shi, Kehang Han, Zhe Wang, Arnaud Doucet, and Michalis K Titsias. Simplified and generalized masked diffusion for discrete data. *arXiv preprint arXiv:2406.04329*, 2024.

- [20] Jacob Devlin, Ming-Wei Chang, Kenton Lee, and Kristina Toutanova. Bert: Pre-training of deep bidirectional transformers for language understanding. *arXiv preprint arXiv:1810.04805*, 2018.
- [21] Emiel Hoogeboom, Alexey A Gritsenko, Jasmijn Bastings, Ben Poole, Rianne van den Berg, and Tim Salimans. Autoregressive diffusion models. *arXiv preprint arXiv:2110.02037*, 2021.
- [22] Daniel T Gillespie. A general method for numerically simulating the stochastic time evolution of coupled chemical reactions. *Journal of computational physics*, 22(4):403–434, 1976.
- [23] Giacomo Zanella. Informed proposals for local mcmc in discrete spaces. *Journal of the American Statistical Association*, 2019.
- [24] Alessandro Barp, Francois-Xavier Briol, Andrew Duncan, Mark Girolami, and Lester Mackey. Minimum stein discrepancy estimators. *Advances in Neural Information Processing Systems*, 32, 2019.
- [25] Jascha Sohl-Dickstein, Peter Battaglino, and Michael R DeWeese. Minimum probability flow learning. In *Proceedings of the 28th International Conference on International Conference on Machine Learning*, pages 905–912, 2011.
- [26] Jiaxin Shi, Yuhao Zhou, Jessica Hwang, Michalis K Titsias, and Lester Mackey. Gradient estimation with discrete stein operators. *arXiv preprint arXiv:2202.09497*, 2022.
- [27] A. A. Barker. Monte carlo calculations of the radial distribution functions for a proton-electron plasma. *Australian Journal of Physics*, 18:119–134, 1965.
- [28] Haoran Sun, Lijun Yu, Bo Dai, Dale Schuurmans, and Hanjun Dai. Score-based continuous-time discrete diffusion models. *arXiv preprint arXiv:2211.16750*, 2022.
- [29] Nikolay Savinov, Junyoung Chung, Mikolaj Binkowski, Erich Elsen, and Aaron van den Oord. Step-unrolled denoising autoencoders for text generation. In *International Conference on Learning Representations*, 2021.
- [30] Huiwen Chang, Han Zhang, Lu Jiang, Ce Liu, and William T Freeman. Maskgit: Masked generative image transformer. In *Proceedings of the IEEE/CVF Conference on Computer Vision and Pattern Recognition*, pages 11315–11325, 2022.
- [31] Jose Lezama, Tim Salimans, Lu Jiang, Huiwen Chang, Jonathan Ho, and Irfan Essa. Discrete predictor-corrector diffusion models for image synthesis. In *International Conference on Learning Representations*, 2022.
- [32] Haoran Sun, Hanjun Dai, Bo Dai, Haomin Zhou, and Dale Schuurmans. Discrete langevin samplers via wasserstein gradient flow. In *International Conference on Artificial Intelligence and Statistics*, pages 6290–6313. PMLR, 2023.
- [33] Michalis K Titsias and Christopher Yau. The hamming ball sampler. *Journal of the American Statistical Association*, 112(520):1598–1611, 2017.
- [34] Will Grathwohl, Kevin Swersky, Milad Hashemi, David Duvenaud, and Chris Maddison. Oops I took a gradient: Scalable sampling for discrete distributions. In *International Conference on Machine Learning*, pages 3831–3841. PMLR, 2021.
- [35] Ruqi Zhang, Xingchao Liu, and Qiang Liu. A langevin-like sampler for discrete distributions. In *International Conference on Machine Learning*, pages 26375–26396. PMLR, 2022.
- [36] David A. Orlando, Charles Y. Lin, Allister Bernard, Jean Y. J. Wang, Joshua E. S. Socolar, Edwin S. Iversen, Alexander J. Hartemink, and Steven B. Haase. Global control of cell-cycle transcription by coupled cdk and network oscillators. *Nature*, 453:944–947, 2008.
- [37] Gavin Kerrigan, Giosue Migliorini, and Padhraic Smyth. Functional flow matching. *arXiv preprint arXiv:2305.17209*, 2023.

A Unifying the TauLDR and score entropy objectives

We first reproduce the TauLDR objective:

$$\mathcal{L}(\theta) = \int \mathbb{E}_{q_t(y)r_t(z|y)} \left[\left\{ \sum_{x' \neq y} \tilde{R}_t^\theta(y, x') \right\} - \left\{ \sum_{z' \neq y} R_t(y, z') \right\} \log(\tilde{R}_t^\theta(z, y)) \right] dt \quad (14)$$

$$= \int \mathbb{E}_{q_t(y)r_t(z|y)} \left[\tilde{R}_t^\theta(y) - R_t(y) \log(\tilde{R}_t^\theta(z, y)) \right] dt, \quad (15)$$

where $R_t(y) \triangleq -R_t(y, y) = \sum_{z' \neq y} R_t(y, z')$. Here r_t represents the probability of a specific transition, given that a transition happens at time t :

$$r_t(z | y) = \begin{cases} \frac{R_t(y, z)}{R_t(y)} & y \neq z \\ 0 & y = z \end{cases} \quad (16)$$

Campbell et al. [9] rewrote the joint distribution :

$$q_t(y)r_t(z | y) = \sum_{x_0} q_0(x_0)\psi_t(z | x_0)\phi_t(y | z, x_0), \quad (17)$$

and then analytically integrate out y to reduce sampling variance, given factorization assumptions on R_t . The downside of this approach is that the resulting loss becomes very complicated and unintuitive.

To circumvent this complication, we propose to instead rewrite the objective with a label switching trick:

$$\mathcal{L}(\theta) = \int \mathbb{E}_{q_0(x_0)q_t(y|x_0)r_t(z|y)} \left[\tilde{R}_t^\theta(y) - R_t(y) \log(\tilde{R}_t^\theta(z, y)) \right] dt \quad (18)$$

$$= \int \mathbb{E}_{q_0(x_0)q_t(y|x_0)} \left[\tilde{R}_t^\theta(y) - \sum_{z \neq y} R_t(y, z) \log(\tilde{R}_t^\theta(z, y)) \right] dt \quad (19)$$

$$= \int \mathbb{E}_{q_0(x_0)q_t(y|x_0)} \left[\sum_{z \neq y} \tilde{R}_t^\theta(y, z) - \sum_{z \neq y} R_t(y, z) \log(\tilde{R}_t^\theta(z, y)) \right] dt \quad (20)$$

$$= \int \mathbb{E}_{q_0(x_0)} \left[\sum_y \sum_{z \neq y} \left\{ q_t(y | x_0) \tilde{R}_t^\theta(y, z) - q_t(y | x_0) R_t(y, z) \log(\tilde{R}_t^\theta(z, y)) \right\} \right] dt \quad (21)$$

$$= \int \mathbb{E}_{q_0(x_0)} \left[\sum_y \sum_{z \neq y} \left\{ q_t(y | x_0) \tilde{R}_t^\theta(y, z) - q_t(z | x_0) R_t(z, y) \log(\tilde{R}_t^\theta(y, z)) \right\} \right] dt \quad (22)$$

$$= \int \mathbb{E}_{q_0(x_0)q_t(y|x_0)} \left[\sum_{z \neq y} \left\{ \tilde{R}_t^\theta(y, z) - R_t(z, y) \frac{q_t(z | x_0)}{q_t(y | x_0)} \log(\tilde{R}_t^\theta(y, z)) \right\} \right] dt \quad (23)$$

$$= \int \mathbb{E}_{q_0(x_0)q_t(y|x_0)} \left[\sum_{x \neq y} \left\{ \tilde{R}_t^\theta(y, x) - \tilde{R}_{t|0}(y, x) \log(\tilde{R}_t^\theta(y, x)) \right\} \right] dt, \quad (24)$$

where $\tilde{R}_{t|0}(y, x) \equiv R_t(x, y) \frac{q_t(x|x_0)}{q_t(y|x_0)}$ is the true reverse transition rate conditioned on x_0 . Note that we switched the labels y and z on line (22). We also renamed z to x on the last line to preserve alphabetical order of the variables for readability. Now we have a simple Monte Carlo estimator for this objective: we just need to sample y from the marginal distribution, and then evaluate the parameterized transition model $\tilde{R}_t^\theta(y, x)$ for all neighbors x of y , which can be done using only one model evaluation.

Note again that we can use the score parameterization for the reverse process:

$$\tilde{R}_t^\theta(z, y) = R_t(y, z) s_t^\theta(z, y). \quad (25)$$

Plugging this parameterization into (24) and absorbing constant terms into C , we get the diffusion weighted denoising score entropy objective (Theorem 3.6 of Lou et al. [13]):

$$\mathcal{L}_{DSE} = \int \mathbb{E}_{q_0(x_0)q_t(y|x_0)} \left[R_t(x, y) \sum_{x \neq y} \left\{ s_t^\theta(y, x) - \frac{q_t(x | x_0)}{q_t(y | x_0)} \log(s_t^\theta(y, x)) \right\} \right] + C dt. \quad (26)$$

B Pseudocode for k -Gillespie’s Algorithm

We give pseudocode for the k -Gillespie’s algorithm presented in Section 3.1 in Algorithm 1. Note that here we use the generation operator $x = G_n^d(y)$ to represent the sequence obtained by changing the d th component of y to the token n .

Algorithm 1 k -Gillespie’s Algorithm with Corrector Steps

Require: $\hat{R}, R^c, t_{min}, \theta$, number of updates K , number of corrector steps C

- 1: Initialize time $t \leftarrow 1$
 - 2: Initialize sample $x \leftarrow \text{MASK}^D$
 - 3: **for** $j = 1$ to D **do**
 - 4: Compute backward rate $r_i^d = \hat{R}_t^\theta(x, G_i^d(x))$
 - 5: Calculate total rate $r^d = \sum_{i \neq x^d} r_i^d$
 - 6: Sample holding time $\tau^d \sim \text{Exp}(r^d)$
 - 7: // Make multiple state transitions
 - 8: **for** $k = 1$ to K **do**
 - 9: Get dimension of transition $d^* = \text{SORTED}(\tau^d)[k]$
 - 10: Update state $x^{d^*} \leftarrow \text{Cat}(\mathbf{r}^{d^*})$ where $\mathbf{r}^{d^*} = \frac{1}{r^{d^*}}(r_1^{d^*}, \dots, r_S^{d^*})$
 - 11: **end for**
 - 12: Update time $t \leftarrow t - \tau^{d^*}$
 - 13: **break** if $t \leq t_{min}$
 - 14: // Apply corrector steps
 - 15: **for** $c = 1$ to C **do**
 - 16: Compute corrector rate $r^c = R_t^c(x, \cdot)$
 - 17: Apply corrector $x \leftarrow \text{POSSIONUPDATE}(x, r^c)$
 - 18: **end for**
 - 19: **end for**
 - 20: Find most likely values for the ungenerated dimensions $x \leftarrow \arg \max_{x_0} p_t^\theta(x_0 | x)$
 - 21: **return** x
-